Journal Name

ARTICLE

Hybrid Elastin-Like Recombinamer-Fibrin Gels: Physical characterization and in vitro evaluation for cardiovascular tissue engineering applications.

Received 00th January 20xx,
Accepted 00th January 20xx

DOI: 10.1039/x0xx00000x

www.rsc.org/

Israel González de Torre[a,c], Miriam Weber[b], Luis Quintanilla[a], Matilde Alonso[a], Stefan Jockenhoevel[b], José Carlos Rodríguez Cabello[b], Petra Mela[b]

In the field of tissue engineering, the properties of the scaffolds are of crucial importance for the success of the application. Hybrid materials combine properties of the different components that constitute them. In this study hybrid gels of elastin-like recombinamer (ELR) and fibrin were prepared with a range on polymer concentrations and ELR-to-fibrin ratios. The correlation between SEM micrographs, porosity, swelling ratio and rheological properties was discussed and a poroelastic mechanism was suggested to explain the mechanical behavior of the hybrid gels. Applicability as scaffold material for cardiovascular tissue engineering was shown by the realization of cell-laden matrixes which supported the synthesis of collagens as revealed by immunohistochemical analysis. As a proof of concept, a tissue-engineered heart valve was fabricated by injection moulding and cultivated in a bioreactor for 3 weeks under dynamic conditions. Tissue analysis revealed production of collagen I and III, fundamental proteins for cardiovascular constructs.

1. Introduction

Tissue engineering applications rely on the scaffold material which should fulfill some properties such as biocompatibility, in some cases biodegradation, absence of toxic byproducts, suitable biomechanical properties and cell-friendly behavior. Thus, the biomaterial scientists are continuously bringing to light new systems to match the requirements of the specific application of interest. The fact that the extra cellular matrix (ECM) consists of several types of materials that provide different properties to the global system suggests that artificial ECMs formed by multiple materials (hybrids)[1-4] might provide a better cellular environment than scaffolds formed only by a single material. In this line, we have realized a hybrid material recapitulating the properties of Elastin-Like Recombinamers (ELRs) and fibrin gels.

ELRs are a kind of protean biomaterial which mimic certain sequences of the natural elastin; they show extraordinary properties for the most cutting-edge applications in biomedicine and nanotechnology[5, 6]. These protein-based polymers are obtained by recombinant DNA technologies with a complete control on their structure and aminoacid sequences. ELRs can include different bioactive sequences[5], such as those governing cell adhesion and protease sensitiveness. They exhibit outstanding biocompatibility, tunable mechanical properties, thermosensitive behavior and strong self-assembly capabilities[5, 6]. The thermosensitive behavior is characterized by a critical temperature in aqueous solution, the transition temperature (T_t), which is associated with a conformational reorganization at the molecular level. Thus, whereas the polymer chains are soluble in water below the T_t, above this temperature they self-assemble into nano- and micro-aggregates and become insoluble in a completely reversible process.

Fibrin has been extensively physically and biologically described[7, 8], and its potential as scaffold material for regenerative medicine and tissue engineering has been shown for cartilage repair[8], nerve regeneration[9], soft tissues reconstruction[10], cardiovascular tissue engineering[11], cell culture and differentiation[12]. It is a natural polymer with several advantages such as autologous origin[13], rapid polymerization, tunable degradation via protease inhibitors[14] and manufacturability into 3D structures[11].

The goal of this work was to incorporate into the fibrin gels, through recombinant elastin (ELRs), some of the features of natural elastin such as elasticity, which is of fundamental importance for many tissues. For cardiovascular tissue engineering applications, and specifically for heart valve tissue engineering, the presence of elasticity is essential for long-term functionality, howeverit is known that little if any functional elastin is synthesised in the constructs under in vitro conditions[15, 16]. Besides improving the mechanical properties, ELRs contribute also the possibility for tailored biofunctionality and reduced thrombogenicity[17].

[a] BIOFORGE, CIBER-BBN, Campus "Miguel Delibes" Edificio LUCIA, Universidad de Valladolid, Paseo Belén 19, 47011, Valladolid, Spain.
[b] Tissue Engineering and Textile Implants, AME, Helmholtz Institute, RWTH, Pauwelsstr. 20, 52074 Aachen, Germany.
[c] TECHNICAL PROTEINS NANOBIOTECHNOLOGY S.L., Campus "Miguel Delibes" Edificio CTTA, Universidad de Valladolid, Paseo Belén 9A, 47011, Valladolid, Spain.

The affinity of fibrinogen and fibrin for native elastin was investigated by Rabaud et al[18] and the potential uses of these materials for tissue engineering have been reported[19-21]. Because of intensive chemical and enzymatic treatments necessary to isolate and purify elastin from natural tissues[22, 23] we propose the use of recombinant elastin bearing lysine groups to promote a covalent reaction with the glutamines from fibrin to obtain hybrid gels. Specifically, we use an ELR, which bears lysines homogeneously distributed along the polypeptide chain and RGD adhesion sequences to increase the number of cell adhesion points provided by fibrin. This ELR is cross-linked with fibrinogen in presence of $CaCl_2$ and thrombin in an enzyme-mediated reaction.

The gels were characterized in terms of mechanical viscoelastic properties. A biphasic poro-viscoelastic (BPVE) model[24-26], which takes into account the viscoelastic behavior generated by both the flow-dependent frictional interactions (poroelasticity) as well as the intrinsic (fluid-independent) viscoelastic nature of the porous solid-matrix, was proposed.

The use of the hybrid ELR-FGs as scaffold for tissue engineering was evaluated in static culture and under dynamic cultivation in the form of a heart valve.

2. Experimental

2.1 Materials

Human fibrinogen (Calbiochem, Darmstadt, Germany) was dissolved in purified water (Milli-Q™; Millipore, Schwalbach, Germany) and dialyzed with a cut-off membrane (Novodirect, Kelh, Germany) of 6,000-8,000 MW overnight against tris-buffered saline (TBS). After sterile filtration the fibrinogen concentration was determined by measuring the absorbance at 280 nm with a spectrophotometer (Spectronic GenesysTM 6; Thermo Fisher Scientific GmbH, Dreieich, Germany).

ELR bioproduction: The ELR used in this study (HRGD6) was constructed using standard genetic engineering techniques and purified using several cycles of temperature-dependent reversible precipitation under and above its transition temperature, as described by by Costa et al[27] and its aminoacid sequence is:

MGSSHHHHHHSSGLVPRGSHMESLLP[(VPGIG)$_2$(VPGKG)(VPGIG)$_2$]$_2$AVTGRGDSPASS[(VPGIG)$_2$(VPGKG)(VPGIG)$_2$]$_2$.

The obtained ELR was then dialyzed against ultra-pure water.

ELRs-Fibrin hybrid gels formation: Two solutions were prepared for the ELR-FGs formation. One containing fibrinogen and HRGD6 at a 1:1 weight ratio in TBS, and a second solution containing a 30% of thrombin and 30% of $CaCl_2$ in TBS. Equal volumes of the two solutions were simultaneously injected, using a two-syringe system equipped with a mixing tip, into the mold and kept at room temperature (r.t.) for at least 15 minutes. After this period, the gel was already formed and could be easily handled. Following this procedure gels with concentrations of 2.5, 5 and 10 mg/mL were prepared.

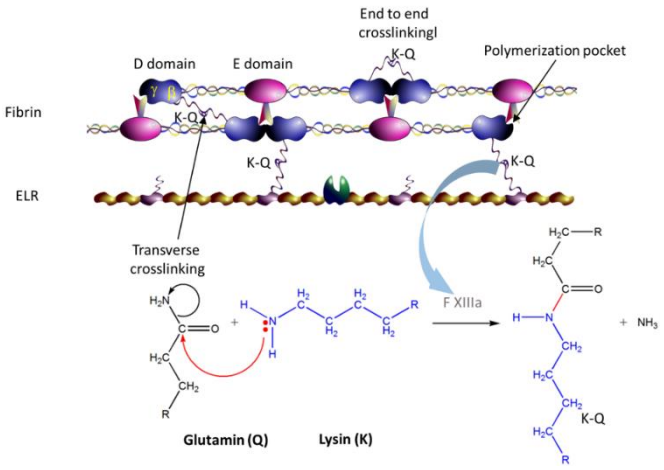

Fig. 1. Scheme of ELRs-Fibrin hybrid gels formation.

The enzymatic process to obtain the ELRs-Fibrin hybrid gels is outlined in Fig 1. The reaction between γ-carboxy-amine group of a glutamine residue and the ε-amino group of a lysine residue is catalyzed by the presence of the enzyme transglutaminase (Factor XIII) which is a Ca^{2+}-dependent enzyme.

At least three replicates for each hybrid gels of each concentration were prepared and measured by any of the instrumental methods reported in this work.

2.1 Experimental methods

Scanning electron microscopy: Scanning electron microscopy (SEM) was employed to investigate the morphology of fibrin and hybrid gels. Fully hydrated gels were dropped into liquid nitrogen, physically fractured, and immersed into liquid nitrogen again. Finally, they were freeze-dried. Images of lyophilized hydrogels were obtained by (FEI Quanta 200 FEG) with no prior coating procedures. SEM in low vacuum mode (~ 1 torr) and with water vapour as working gas was used to investigate the morphology of all hydrogels.

Differential Scanning Calorimetry (DSC) measurements: DSC experiments were performed on a Mettler Toledo 822e DSC with a liquid nitrogen cooler accessory. Both temperature and enthalpy were calibrated with an indium standard at the same experimental conditions used for the studied materials. TBS solutions of ELRs and ELR-FGs at 10 mg mL-1 were prepared. In a typical DSC run, 20 µL of the solution was placed inside a standard 40 µL aluminium pan hermetically sealed. The same volume of TBS was placed in the reference pan. As for ELR-FGs analysis, 20 mg of the hydrated hydrogel was placed in the sample pan. To account for the exact amount of polymer in the assayed hydrogel, the sample was lyophilized and weighted

after DSC run. All samples were equilibrated for 10 min at 0ºC inside the sample chamber just before the beginning of each experiment, and then, heated from 0 to 50 ºC at a heating rate of 5ºC/min. The scans were run under a nitrogen atmosphere.

Porosity calculations and swelling ratio: Cylindrically shaped hydrogels were prepare for mechanical and physical characterizations.

The following equation[28] was employed to estimate hydrogel porosity:

$$\text{Porosity (\%)} = ((W_1-W_2)/\rho_{water})x100/V_{hydrogel} \quad \text{(Eq.1)}$$

where W_1 and W_2 are the weight of the swollen and lyophilized gels, respectively, ρ_{water} is the density of pure water, and $V_{hydrogel}$ is the measured volume of the gel in the swollen state ($V_{hydrogel} = \pi r^2 h$, where r and h are the radius and height of the cylindrical sample, respectively). Excess surface water was removed with a filter paper before each measurement.

The change of the volume of the hydrogels in aqueous solution, related to the ELR phase-transition, was quantified at a fixed temperature in terms of the equilibrium swelling ratio by weight, Q_w, defined as

$$Q_w(\%) = ((W_1-W_2)/W_2)x100 \quad \text{(Eq.2)}$$

All measurements were taken 24 h after soaking the hydrogel in MQ water at the selected temperature. Equilibrium was defined as the steady state at which there was no change in volume of the ELR-FGs.

Both porosity and the equilibrium swelling ratio were determined at 4 and 37 °C. Lyophilization (freeze-drying) was performed on fully hydrated hydrogels frozen in liquid nitrogen at the corresponding test temperature.

Rheological measurements: A strain-controlled AR-2000ex rheometer (TA Instruments) was employed to perform rheological experiments. Disc-shaped gel samples were placed between parallel plates of nonporous stainless steel (diameter = 12 mm) and the gap between the plates was adjusted applying the minimum normal force to prevent slippage. A gap higher than 1000 µm was always reached after the sample relaxed until equilibrium. Measurements were performed at 37 °C, with the sample temperature being controlled and maintained using a Peltier device.

Two different measurements were carried out in shear deformation mode. First, the dynamic shear modulus was measured as a function of strain by a dynamic strain sweep with amplitudes ranging between 0.1% and 20% and at a frequency of 1 Hz. This measurement was done to determine the range of strain amplitudes over which the gels exhibited a linear region of viscoelasticity. A second measurement consisted in the dynamic frequency sweep between 0.05 and 70 Hz at a fixed strain, selected within the hydrogel linear region with the aim of obtaining the dependence of the dynamic shear modulus and loss factor on frequency. Rheological evaluation provided the storage modulus (G'), the loss modulus (G''), the complex modulus magnitude $|G^*|$, ($|G^*|^2 = (G')^2 + (G'')^2$), and the loss factor ($\tan\delta \equiv (G'')/(G')$, where δ is the phase angle between the applied stimulus and the corresponding response) as a function of strain amplitude or frequency.

Cytocompatibility: Hybrid ELRs-FGs were prepared with a final polymer concentration of 10 mg/mL (ELR to fibrin ratio 1:1) and 10 million/mL of Ovine Umbilical Smooth Muscle Cells (OUSMCs) in passage 5. For this purpose, a solution of fibrinogen and HRGD6, at the desired proportion, in sterile TBS was prepared. An equal volume of a second solution of 30% thrombin and 30% $CaCl_2$ in TBS was prepared to which OUSMCs were added (20 million/mL). The solutions were injected using a two-syringe system into a 24 well-plate to obtain 0.5 mL ELRs-Fibrin hybrid gels in a concentration of 10 mg/mL of polymer and with 5 million OUSMCs homogeneously embedded.

As control, fibrin gels with a concentration of 10 mg/ml fibrinogen and 10 million/mL OUSMCs were prepared in a similar way as previously described for ELRs-Fibrin hydrogels.

The gels were cultured for 15 days at 37°C and 5% CO_2 in incubator (Binder, Germany) in low glucose DMEM with 10% FCS, antibiotic/antimycotic solution, 1.0mM L-ascorbic acid 2-phosphate (Sigma-Aldrich) and 1,6 µl/ml tranexamic acid (1000mg/ml; Pfizer, Berlin, Germany). Medium was changed every three days. After 15 days, the gels were removed from the well-plate and processed for immunohistochemistry.

Immunohistochemistry: Nonspecific sites on Carnoy's fixed, paraffin-embedded sections from native ovine and tissue-engineered valves were blocked and the cells were permeabilized with 5% NGS (Sigma) in 0.1% triton PBS. Sections were incubated for 1 h at 37°C with the following primary antibodies: 1:1000 mouse anti-a-SMA (A 2547; Sigma); 1:200 rabbit anti-type collagen I (R 1038; Acris); 1:25 rabbit anti-type collagen III (R 1040; Acris); 1:200 rabbit anti-elastin (20RER003;Fitzgerald); and 1:60 rabbit polyclonal anti-human fibrinogen (F0111; Dako). The sections were incubated for 1 h at 37C with either rhodamine or fluorescein-conjugated goat anti-mouse or goat anti-rabbit secondary antibodies: 1:400 mouse a-SMA (A 11008; Molecular Probes); 1:400 rabbit type collagen I (A 11008; Molecular Probes); 1:300 rabbit type collagen III (E 0432; Dako); and 1:400 rabbit elastin (A 11008; Molecular Probes). Type collagen III signal was amplified by an additional incubation with 1:1000 streptavidin/TRITC (RA 021; Acris). The native ovine mitral valve served as a positive control. As negative controls, samples were incubated in diluent with the second antibody only. Tissue sections were counterstained with DAPI nuclei acid stain (Molecular Probes). Samples were observed with a microscope equipped for epi-illumination (AxioObserver Z1; Carl Zeiss GmbH). Images were acquired using a digital camera (AxioCam MRm; Carl Zeiss GmbH).

Aortic valve fabrication and bioreactor conditioning: A sterile solution of fibrinogen and HRGD6 in TBS was prepared (20 mg/mL of fibrinogen and 20 mg/mL of HRGD6 in 3 mL of TBS).

A solution of 30% of thrombin and 30% of $CaCl_2$ in sterile TBS was prepared (3 mL) (final concentrations: fibrinogen-ELR 10 mg/mL, thrombin 15%, $CaCl_2$ 15%).

60 millions of miofibroblasts were suspended into the thrombin/$CaCl_2$ sterile solution. A sterilized aortic valve mould of 19 mm was used to cast the valve. The mould sterilization was performed using a low-temperature hydrogen peroxide gas plasma (STERRADs 100S Sterilization System, ASP, Norderstedt, Germany) one week before use it. A warp-knitted textile mesh was stitched up to a silicon ring, which was placed inside the mould. Both solutions were simultaneously injected into the mould; once the solutions were mixed inside the mould with the cells, the mould was quickly closed to avoid any leaking, and this was kept closed at r.t., under sterile conditions for 45 minutes. Next, the valve was removed from the mould and was placed into a bioreactor. The valves were cultured in low glucose DMEM with 10% FCS, antibiotic/antimycotic solution, 1.0mM L-ascorbic acid 2-phosphate (Sigma-Aldrich) and 1,6 µl/ml tranexamic acid (1000mg/ml; Pfizer, Berlin, Germany). Culture medium within the bioreactor was replaced after seven days. Culture conditions were monitored by measuring lactate, glucose, pO2, pCO2, and pH levels on a blood-gas analyzer (Blood gas analyzer ABL 800 Flex, Radiometer, Copenhagen, Denmark). Finally, the valve was removed from the bioreactor under sterile conditions. The leaflets were opened with the help of a scalpel and placed in a bioreactor for dynamic cultivation cycle of fifteen days was started. Culture medium was replaced every seven days. The stimulation program was based on the procedure described by Weber et al[29]. The starting parameters of the dynamic cultivation were set at a frequency of 20 beats per minute (bpm). BGA analyses were carried out every two days. After two days of stimulation, the frequency was raised till 40 bpm. Medium was changed after one week. After fifteen days the bioreactor medium was removed from the bioreactor and the valve was extracted from the bioreactor.

Tissue samples were obtained from the leaflets and from the wall of the valve and prepared for immunohistochemistry.

Statistical analysis: Values are reported as mean ± SD ($n \geq 3$). Statistical analysis was evaluated by one way analysis of variance using the Holm-Sidak method. A p value lower than 0.05 was considered to be statistically significant. (**) $p < 0.001$, (*) $p < 0.05$. $p>0.05$ indicates no significant differences (n.s.d.).

3. Results and discussion

3.1 Rheological characterization.

The linear viscoelastic region of the hydrogel was determined by using strain sweep measurements. This region reaches a strain of 6-7% (Fig. 2). Then, a 1% strain was selected to carry out several dynamic frequency sweep measurements.

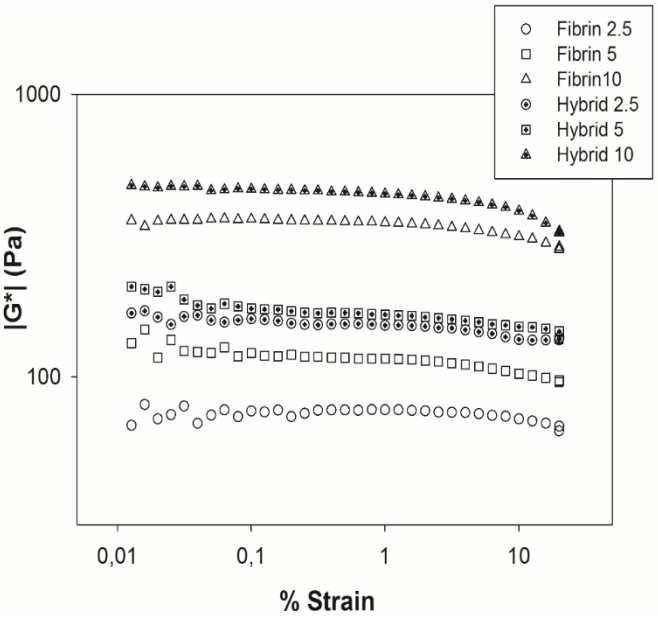

Fig. 2. Complex module magnitude at a frequency of 1 Hz as a function of strain amplitude for fibrin gels (hollow symbols) and ELR-FGs (cross hair symbols). Each curve corresponds to the average of three different samples.

The optimal ELR to fibrin ratio in the hydrogel was selected as the one with the maximum |G*| while maintaining an elastic behaviour (G´>>G´´ and a low value of δ). As can be seen in Fig. 3, this criterion is satisfied for an ELR percentage of 50%. This ratio resulted in G´= 500 Pa, G´´ = 30 Pa, and δ = 3° at 1 Hz. These values indicate a high elastic behaviour of hydrogels. Therefore, gels with a 1:1 ratio of ELR to fibrin were used in the rest of the work.

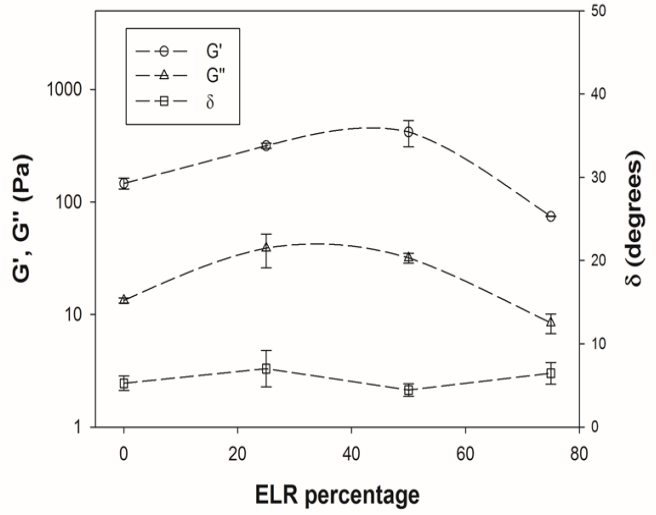

Fig. 3. Evolution of storage (G') and loss (G'') moduli, and δ as function of the ELRs proportion in hybrid ELR-FGs at a frequency of 1 Hz. These values were obtained from dynamic frequency sweeps at 37°C using a strain amplitude of 1%.

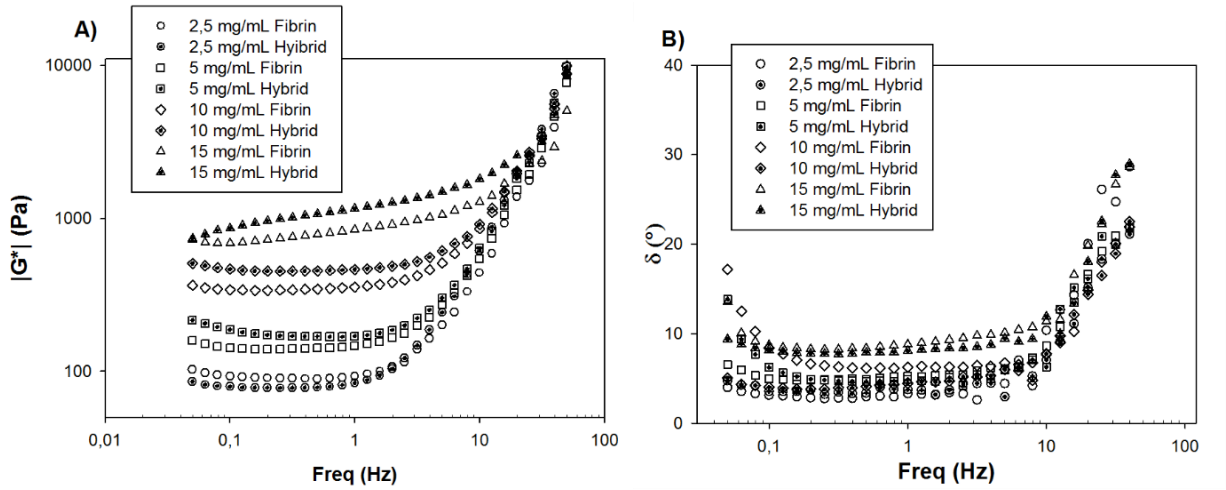

Fig. 4. Evolution of complex modulus magnitude, A), and phase angle (δ), B), as function of the frequency for several concentrations of hybrid ELR-FGs (cross hair symbols) and fibrin gels (hollow symbols). Each curve corresponds to the average of three different samples.

Fig. 5 shows the storage and loss moduli along with the phase angle as a function of the ELR concentration at a fixed frequency (1 Hz). Both G´ and G´´ (Fig. 5 (A) and (B) respectively) increased with an increasing concentration with G´ >> G´´ at concentration higher than 5 mg/mL (p>0.001) These results agree with bibliography since Sun et al.[30] have reported an increase of G´ with the fibrin concentration in fibrin hydrogels.

As far as δ is concerned (Fig. 5 (C)), an increase with concentration is found for both types of hydrogels. Anyway, the low values obtained are in agreement with a high elastic hydrogel behaviour throughout the concentration range considered. In conclusion, the presence of ELRs in the hybrid gels increases the mechanical properties of these gels with respect to the fibrin gels.

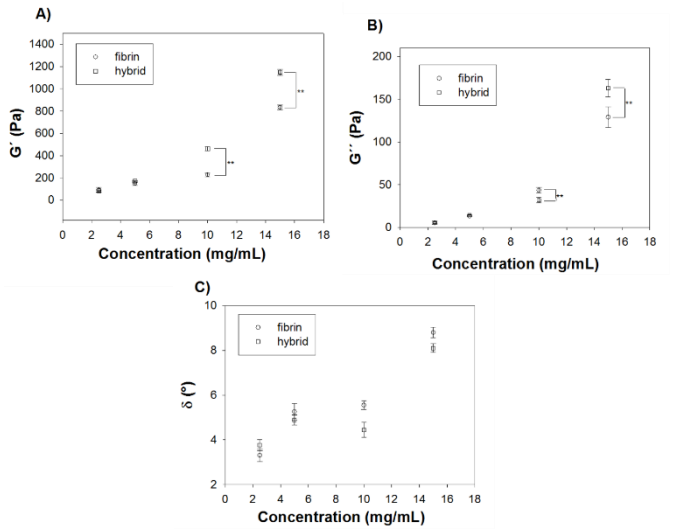

Fig. 5. Evolution of G', G'' and for Fibrin gels (circles) and ELR-FGs (squares) as function of the recombinamer concentration at 37°C.

To provide an insight in the physical mechanisms that determines the frequency dependence of |G*|, the evolution of |G*| was plotted as a function of $f^{1/2}$ (Fig. 6). For 2.5 and 5 mg/mL concentrations, a plateau in |G*| values was observed up to about 1 $Hz^{1/2}$. However, for higher concentrations, a linear dependence of |G*| on $f^{1/2}$ was found. A similar behaviour was recently reported for Elastin-Like Catalyst Free Click Gels[31] where this linear dependence was related to a poroelastic mechanism that dominates the viscoelastic behaviour in this frequency range. The slope is related to the gel permeability that is a macroscopic measure of the ease with which a fluid can flow through the gel matrix. When the ELRs concentration increases, permeability decreases[32].

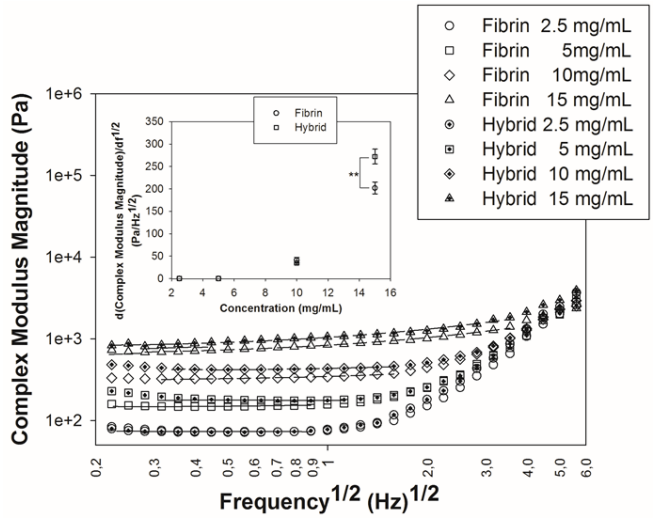

Fig. 6. Dependence of the magnitude of the complex modulus on f½ at 37°C for every kind of gel and concentration analysed in this work. The dashed line corresponds to the least-square linear regression of the linear region. In every case R2 is always better than 0.990. The slope of these curves is plotted in the inset as a function of concentration in the range 2.5–15 mg/mL. Each curve corresponds to the average of three different samples measured.

For the concentration of 15 mg/mL a higher slope is found for the ELR-FGs, corresponding to a higher hindrance in the fluid flow through the gel structure. These results obtained from the rheological measurements will be correlated with SEM micrographs in its corresponding sub-section.

3.2 Thermosensitive behaviour

ELRs exhibit some thermal properties which make them very interesting polymers for biomedical applications. One of these properties is the temperature sensitiveness, characterized by the T_t. Below this temperature, the polymeric chains of the ELRs undergo a hydrophobic hydration, which means that the ELRs chains are completely hydrated by clathrates formed by water molecules. Above T_t, the chains of ELRs adopt a more ordered structure excluding the water that forms those clathrates and precipitate. The thermal sensitiveness was present in the hybrid gels as shown by DSC and organoleptic observations. Disc-shaped hybrid gels (10 mg/mL, 12 mm diameter and 3 mm high) were formed .and immersed in cold distilled water (4°C) for one minute. Then, the gels were partially immersed in a warm distilled water (37°C) for one minute. A change in the transparency of the gels was clearly evident as can be observed in the picture sequence of the Fig. 7 (A, B). This thermosensitive behaviour was corroborated by DSC measurements, which showed an increment in the T_t of the hybrid gel with respect to the ELR of more than 5°C. Therefore, the thermosensitive properties of the ELRs have inherited by our hybrid gels.

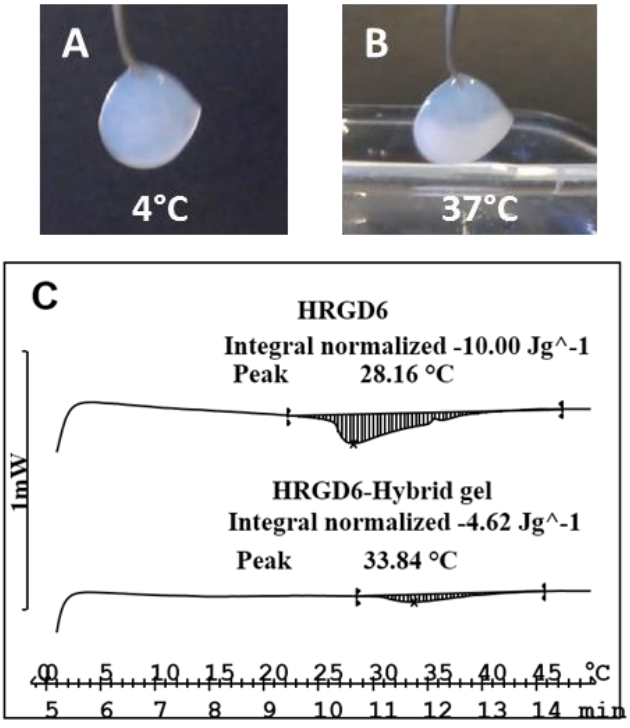

Fig. 7. Thermosensitive behaviour of the ELR-FGs. (A) Hybrid ELR-FG after 1 minute at 4°C. (B) Hybrid ELR-FG after partial immersion in water at 37°C for 1 minute. The gel had a more opaque appearance when it was exposed to a temperature higher that Tt. (C) Thermogram of ELR (10 mg/mL) (upper curve) and ELR-FG (10 mg/mL) (lower curve) in purified water.

3.3 Microscopic structure

SEM micrographs of hybrid gels with different polymer concentrations are shown in Fig. 8.

Fibrin gels showed a compact fibrin network microstructure for a concentration of 10mg/ml (Fig. 8 (E)).

Hybrid gels showed a microscopic structure where the mixture of both biopolymers is evident. For the lowest concentration (2.5 mg/mL, Fig. 8 (A)) fibrin strands are clearly observed. Moreover, thin elastin fibres can be also found, and some of them are in the perpendicular direction to the fibrin strands. A significant pore size of several microns must be noted. When concentration increases (5 mg/mL, Fig. 8 (B)), a similar structure is detected, but fibrin strands are closer and the elastin fibres give rise to a web-like structure. Finally, for higher concentration (10 and 15 mg/mL, Fig. 8 (C and D)) a mesh-like structure and a pore size reduction is observed.

SEM micrographs confirm the higher hindrance in the fluid flow through the gel structure suggested from rheological measurements (see inset in Fig. 6) owing to the decrease in the pore size and more compact structure when the polymers concentration increases.

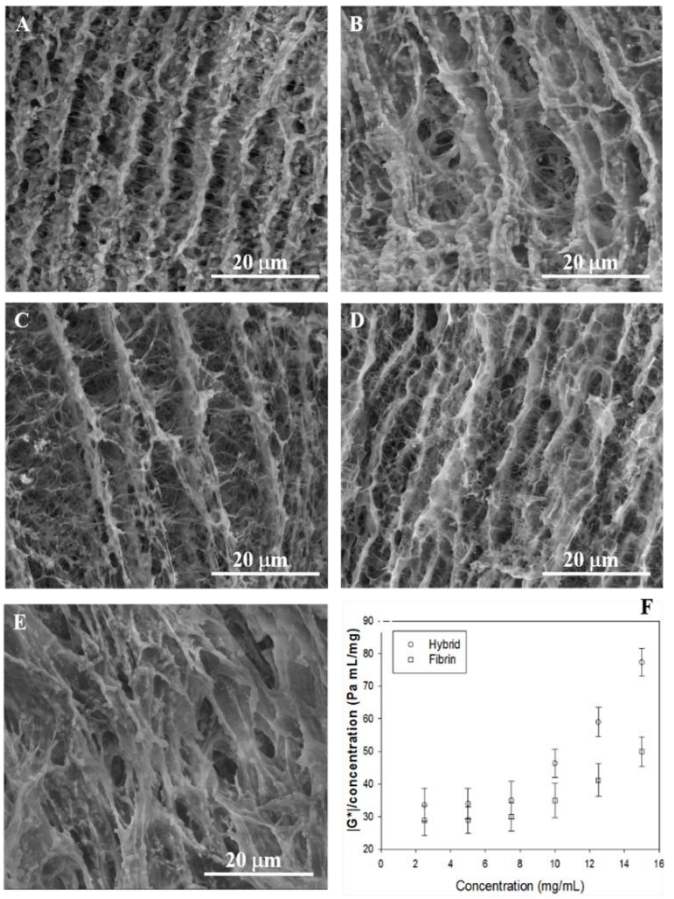

Fig 8. SEM pictures of ELR-FGs for concentrations 2.5, 5, 10 and 15 mg/mL (A, B, C, D), at several magnifications. Fibrin gel control of 10 mg/mL (E). Variation of the concentration-normalized |G*| versus concentration for ELR-FGs (circles) and fibrin gels (squares). A 1% strain amplitude and a frequency of 1 Hz were used for the rheological measurements (F).

Fig. 8 (F) shows the concentration-normalized complex modulus magnitude (|G*|/concentration) as a function of the polymer concentration for the fibrin and the hybrid gels. Both curves show a similar behaviour. Two regions are detected in the graphs. First, a plateau for concentrations lower than 10 mg/mL with similar values for the fibrin and hybrid gels. Second, for higher concentrations a significant increase of the concentration-normalized complex modulus magnitude is observed, higher for the hybrid gel. Therefore, a synergetic interaction between fibrin and elastin can be suggested for these concentrations.

To provide a comprehensive overview of the microscopic structure of the ELR-FGs, porosity values and swelling ratios were determined. Fig. 9 (A) shows the dependence of the porosity of the hybrid gels as a function of concentration. Porosity decreased when concentration increased at both temperatures. Porosity at low temperature (4°C) is higher than at normal physiological temperature (37°C). A similar porosity behaviour was already observed for Elastin-Like Recombinamers Catalyst Free Click Gels by González de Torre et al.[32]. In any case, at 4°C and 37°C, these ELR-FGs exhibited a high porosity, which is one of the main factors to improve the flow of nutrients inside the scaffold and to facilitate the cell colonization of the gels[33-35]. The relative swelling ratio ($Q_{4°C}/Q_{37°C}$) for hybrid gels at 4°C and at 37°C is showed in Fig. 9 (B). As could be expected, the relative swelling ratio decreased when concentration increased. One plausible explanation could be that when the concentration increases, the number of polymers chains does, and the number of cross-linked chains increases too. This rising in the number of cross-linked chains produce a reduction in the swelling capability of the gels. These results agree with those found in literature[36].

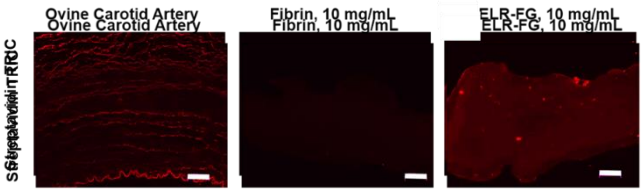

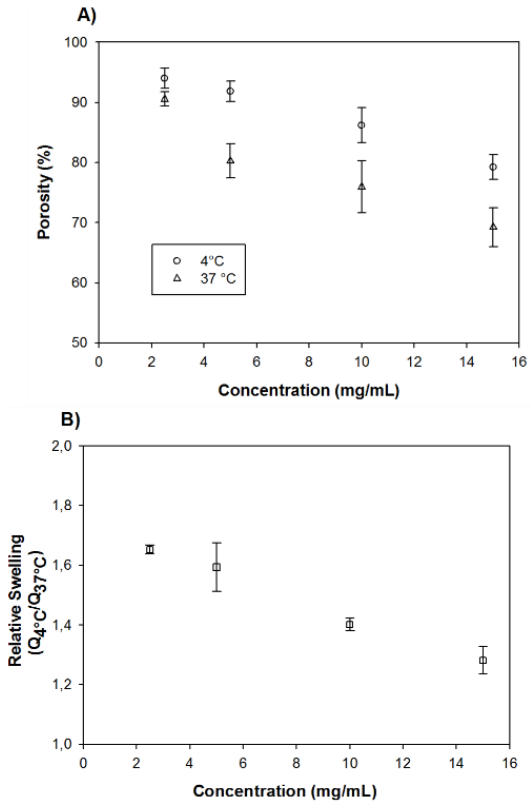

Fig. 9. (A) Porosity of the ELRs-FGs at 4°C and 37 °C. (B) Relative equilibrium swelling ratio, ($Q_{4°C}/Q_{37°C}$) for hybrid gels at 4°C and at 37°C.

Fig. 10. Light microscopy pictures of a piece of ovine carotid artery (control), fibrin gels and ELR-FGs samples stained against elastin Straptavidin TRIC.

The presence of ELRs in the ELR-FGs was corroborated by immunofluorescence staining with streptavidin TRIC (red stain) As can be observed in Fig. 10, natural elastin in ovine carotid artery samples is arranged in thin, ordered layers. In ELR-FGs the presence of ELRs appears as a continuous and homogeneous background, since hybrid gels were formed from homogeneous solutions of fibrin and ELRs where no segregation was observed. The presence of some bright dots indicates agglomerations of unreacted ELRs that adopt a folded structure above their Tt [37, 38]. In the case of fibrin gels, no presence of elastin was found, as expected.

3.4 ELR-FG scaffolds

Polymerization of ELR-FGs in the presence of cells resulted in gels with a homogeneous distribution of cells. Immuohistochemistry stainings showed the cells expressed a-SMA and produced collagen I and III during the 15 days they were kept in static cultivation (Fig. 11). Production of elastin could not be detected and the amorphous background of the

ELR-FGs is attributed to the presence of ELR. During cultivation, levels of glucose, lactate, CO_2, O_2 and pH were monitored and normal values (data not shown) that indicated healthy cells metabolism were recorded.

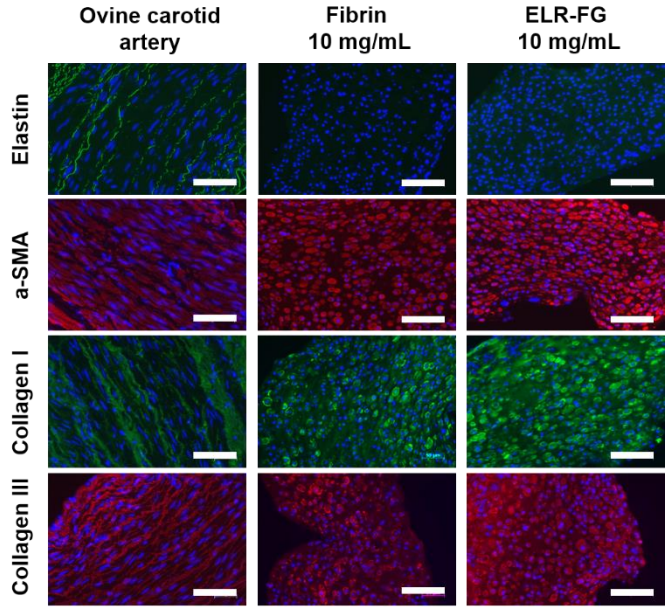

Fig. 11. Elastin, a-SMA, Collagen I and Collagen III immunostaining images for ovine carotid artery (left column, positive control) and 3D cultures of OUSMCs in fibrin and ELR-FGs (center and right column).

3.5 ELR-FG as scaffold for cardiovascular tissue engineering

The potential of the hybrid gels as scaffold for cardiovascular tissue engineering was demonstrated by producing a semilunar heart valve with a molding process (Fig. 12 (A-C)). The sterile molding components (Fig. 12(A)) were assembled (Fig. 12(B)) and the two components forming the hybrid gel were carefully injected (Fig. 12(C)). A silicone ring was used to mechanically support the valve after molding and facilitate handling. The valve was cultivated in static conditions in the closed-leaflet configuration (Fig, 12 (D)) for 1 one week. The leaflet were cut open before placing the valve into the bioreactor for dynamic stimulation (Fig. 12 (E)) where it was conditioned for 2 more weeks with opening and closing cycles (Fig. 12 (F-G))

After one week, the medium was changed. Along this culture time, BGA tests were carried out every two days: the glucose and lactate level started at 5.0 mmol/L and 1.4 mmol/L, respectively, and at the end it was 3.3 mmol/L and 4.8 mmol/L, respectively. pH was kept at 7.35 and CO_2 and O_2 pressures were always around 43 and 150 mmHg respectively. The glucose consumption and the increase of the lactate levels means a normal growing of the OUSMCs. Immunohistochemistry staining showed expression of αSMA (Fig. 13 A, B and C), aligned Collagen I and III were produced, in both wall and leaflets (Fig. 13 D-I). No synthesis of elastin was detected and the gels presented a background staining to be attributed to the ELR as in the case of statically cultivated gels (not shown).

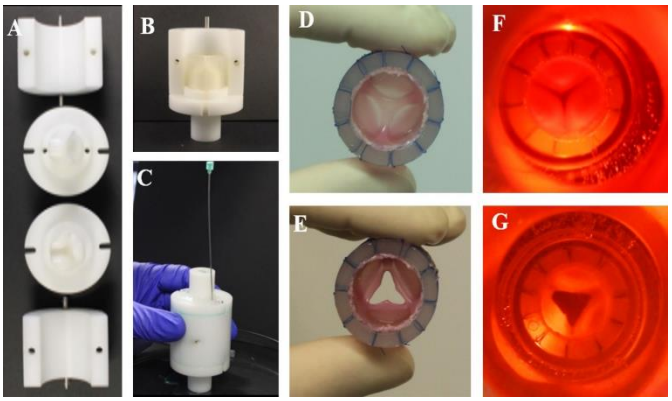

Fig. 12. Semilunar heart valve fabrication and conditioning. A) Mould components; B) in the assembled configuration; C) Polymers injection; Valve after static conditioning before and after leaflets opening (D and E respectively); Valve inside the bioreactor during dynamic conditioning, open (F) and closed (G).

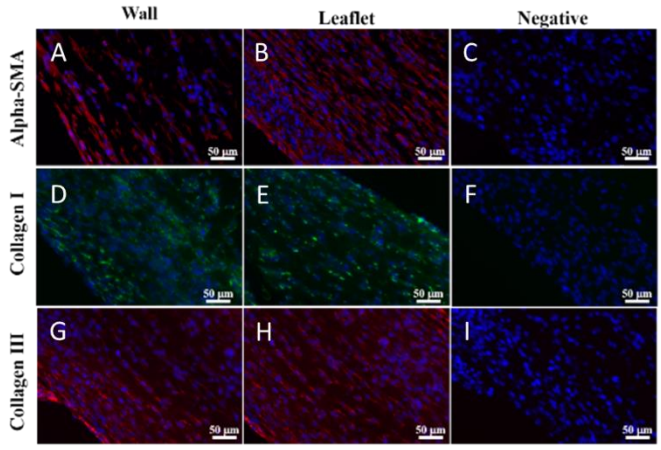

Fig. 13. a-SMA, Collagen I and Collagen III immunostaining images for engineered ELR-FGs aortic valve (leaflets and walls) with OUSMCs. Right column: negative controls.

Conclusions

A new hybrid material formed by Elastin-Like Recombinamers (ELRs) and fibrin was presented. This material is easily formed and handled, and combines the outstanding mechanical properties of the ELRs with the well-known cell-affinity of the fibrin gels[39-42], improving the elastic properties with respect to pure fibrin gels. A poroelastic mechanism dominates the viscoelastic behaviour in the range of the analysed frequencies. The functionality of the hybrid gels can be tailored by choosing an ELR with a desired bioactive sequence, here shown with an ELR bearing he cell adhesion sequence RGD.

This kind of gels exhibits a good cytocompatibility, cells colonized the whole gels and developed their natural structures to build the extra cellular matrix. That is a promising starting point to apply these new ELR-FGs in the field of tissue engineering, here demonstrated with the fabrication of a

semilunar heart valve which was molded and cultivated for a total of 21 days in a bioreactor.

Acknowledgements

We acknowledge financial support from the EU through the European regional development fund (ERDF) NMP3-LA-2011-263363, HEALTH-F4-2011-278557, PITN-GA-2012-317304), FP7/2007-2013/ under REA grant agreement 317512, from the MINECO (MAT-2010-15982, MAT2010-15310, PRI-PIBAR-2011-1403 and MAT2012-38043-C02-01), the JCyL (projects VA152A12-2, VA244U13 and VA155A12-2), the CIBER-BBN, the JCyL and the Instituto de Salud Carlos III under the "Network Center of Regenerative Medicine and Cellular Therapy of Castilla and Leon", the START programme of the Medical Faculty of the RWTH Aachen University (project 691348), the Fördergemeinschaft Deutsche Kinderherzzentren e.V. and the People Programme (Marie Curie Actions) of the European Union's Seventh Framework Programme FP7/2007-2013/ under REA grant agreement n°317512

Notes and references

1 1. A. Tampieri, M. Iafisco, M. Sandri, S. Panseri, C. Cunha, S. Sprio, E. Savini, M. Uhlarz and T. Herrmannsdörfer, *ACS applied materials & interfaces*, 2014, **6**, 15697-15707.
2 2. M. Hoyer, N. Drechsel, M. Meyer, C. Meier, C. Hinüber, A. Breier, J. Hahner, G. Heinrich, C. Rentsch, L. A. A. Garbe, W. Ertel, G. Schulze-Tanzil and A. Lohan, *Materials science & engineering. C, Materials for biological applications*, 2014, **43**, 290-299.
3 3. D. J. Cornwell, B. O. Okesola and D. K. Smith, *Angewandte Chemie (International ed. in English)*, 2014, **53**, 12461-12465.
4 4. M. Farokhi, F. Mottaghitalab, M. A. Shokrgozar, J. Ai, J. Hadjati and M. Azami, *Materials science & engineering. C, Materials for biological applications*, 2014, **35**, 401-410.
5 5. J. C. Rodríguez-Cabello, L. Martín, M. Alonso, F. J. Arias and A. M. Testera, *Polymer*, 2009, **50**, 5159-5169.
6 6. E. R. Wright and V. P. Conticello, *Advanced Drug Delivery Reviews*, 2002, **54**, 1057-1073.
7 7. H. Zhao, L. Ma, J. Zhou, Z. Mao, C. Gao and J. Shen, *Biomedical materials (Bristol, England)*, 2008, **3**, 15001.
8 8. M. Haugh, S. Thorpe, T. Vinardell, C. Buckley and D. Kelly, *Journal of the mechanical behavior of biomedical materials*, 2012, **16**, 66-72.
9 9. V. Carriel, J. Garrido-Gómez, P. Hernández-Cortés, I. Garzón, S. García-García, J. Sáez-Moreno, M. Del Carmen Sánchez-Quevedo, A. Campos and M. Alaminos, *Journal of neural engineering*, 2013, **10**, 26022.
10 10. C. M. Hwang, B. Ay, D. L. Kaplan, J. P. Rubin, K. G. Marra, A. Atala, J. J. Yoo and S. J. Lee, *Biomedical materials (Bristol, England)*, 2013, **8**, 14105.
11 11. S. Jockenhoevel, G. Zund, S. Hoerstrup, K. Chalabi, J. Sachweh, L. Demircan, B. Messmer and M. Turina, *European journal of cardio-thoracic surgery : official journal of the European Association for Cardio-thoracic Surgery*, 2001, **19**, 424-430.
12 12. S. Willerth, T. Faxel, D. Gottlieb and S. Sakiyama-Elbert, *Stem cells (Dayton, Ohio)*, 2007, **25**, 2235-2244.
13 13. M. Dietrich, J. Heselhaus, J. Wozniak, S. Weinandy, P. Mela, B. Tschoeke, T. Schmitz-Rode and S. Jockenhoevel, *Tissue Eng Part C Methods*, 2013, **19**, 216-226.
14 14. E. Cholewinski, M. Dietrich, T. C. Flanagan, T. Schmitz-Rode and S. Jockenhoevel, *Tissue engineering. Part A*, 2009, **15**, 3645-3653.
15 15. A. Patel, B. Fine, M. Sandig and K. Mequanint, *Cardiovascular research*, 2006, **71**, 40-49.
16 16. A. Mol, A. I. Smits, C. V. Bouten and F. P. Baaijens, *Expert Review of Medical Devices*, 2009, **6**, 259-275.
17 17. I. Gonzálezde Torre, F. Wolf, M. Santos, L. Rongen, M. Alonso, S. Jockenhoevel, J. C. Rodríguez-Cabello and P. Mela, *Acta Biomaterialia*, 2015, **12**, 146-155.
18 18. M. Rabaud, F. Lefebvre, Y. Piquet, F. Belloc, J. Chevaleyre, M. Roudaut and H. Bricaud, *Thrombosis research*, 1986, **43**, 205-211.
19 19. F. San-Galli, C. Deminière, J. Guérin and M. Rabaud, *Biomaterials*, 1996, **17**, 1081-1085.
20 20. M. Riquet, F. Carnot, P. Gallix, D. Callise, F. Lefebvre and M. Rabaud, *Biomaterials*, 1990, **11**, 518-520.
21 21. N. Bonzon, X. Carrat, C. Deminiére, G. Daculsi, F. Lefebvre and M. Rabaud, *Biomaterials*, 1995, **16**, 881-885.
22 22. R. P. Mecham, *Methods (San Diego, Calif.)*, 2008, **45**, 32-41.
23 23. S. W. Jordan, C. A. Haller, R. E. Sallach, R. P. Apkarian, S. R. Hanson and E. L. Chaikof, *Biomaterials*, 2007, **28**, 1191-1197.
24 24. A. F. Mak, *J Biomech Eng*, 1986, **108**, 123-130.
25 25. A. F. Mak, *Biorheology*, 1986, **23**, 371-383.
26 26. S. Kalyanam, R. D. Yapp and M. F. Insana, *J Biomech Eng*, 2009, **131**, 081005.
27 27. R. Costa, C. Custódio, F. Arias, J. Rodríguez-Cabello and J. Mano, *Small (Weinheim an der Bergstrasse, Germany)*, 2011, **7**, 2640-2649.
28 28. X. Zeng and E. Ruckenstein, *Industrial & Engineering Chemistry Research*, 1996, **35**, 4169-4175.
29 29. M. Weber, E. Heta, R. Moreira, V. N. Gesche, T. Schermer, J. Frese, S. Jockenhoevel and P. Mela, *Tissue engineering. Part C, Methods*, 2014, **20**, 265-275.
30 30. Y. Sun, O. Giraudier and V. L. Garde, *Biopolymers*, 2005, **77**, 257-263.
31 31. I. González de Torre, M. Santos, L. Quintanilla, A. Testera, M. Alonso and J. C. Rodríguez Cabello, *Acta Biomaterialia*, 2014, **10**, 2495-2505.
32 32. I. González de Torre, M. Santos, L. Quintanilla, A. Testera, M. Alonso and J. C. Rodríguez Cabello, *Acta Biomaterialia*, 2014.
33 33. B. Lawrence and S. Madihally, *Cell adhesion & migration*, 2008, **2**, 9-16.
34 34. E. Pamula, L. Bacakova, E. Filova, J. Buczynska, P. Dobrzynski, L. Noskova and L. Grausova, *Journal of materials science. Materials in medicine*, 2008, **19**, 425-435.
35 35. G. Chan and D. Mooney, *Trends in biotechnology*, 2008, **26**, 382-392.
36 36. K. Trabbic-Carlson, L. A. Setton and A. Chilkoti, *Biomacromolecules*, 2003, **4**, 572-580.
37 37. J. C. Rodríguez-Cabello, J. Reguera, A. Girotti, M. Alonso and A. M. Testera, *Progress in Polymer Science*, 2005, **30**, 1119-1145.
38 38. P. Schmidt, J. Dybal, J. C. Rodriguez-Cabello and V. Reboto, *Biomacromolecules*, 2005, **6**, 697-706.
39 39. R. Rosser, W. Roberts and J. Ferry, *Biophysical chemistry*, 1977, **7**, 153-157.
40 40. G. Nelb, C. Gerth and J. Ferry, *Biophysical chemistry*, 1976, **5**, 377-387.
41 41. C. Gerth, W. Roberts and J. Ferry, *Biophysical chemistry*, 1974, **2**, 208-217.
42 42. W. Roberts, O. Kramer, R. Rosser, F. Nestler and J. Ferry, *Biophysical chemistry*, 1974, **1**, 152-160.